

Full Length Research Paper

Uranium mineralizations of Wadi Sikait mylonites, Southeastern Desert, Egypt

G. M. Saleh*, S. A. Abdallah, A. A. Abbas, N. A. Dawood and M. A. Rashed

Nuclear Materials Authority, Cairo, P. O. Box 530 El Maadi, Egypt.

Accepted 4 January, 2011

This article deals with mineralizations and spectrometric study as well as geology and geochemistry of the late Pan-African cataclastic rocks (mylonites) of Wadi Sikait area. The area is composed of metagabbros, ophiolitic mélange, metasediments, mylonitic rocks, porphyritic biotite granites, leucogranites and lamprophyre dykes. The mineralogical study of the mylonitic samples revealed the presence of uranothorite, thorite, boltwoodite and niobium minerals (ferroclombite, ishikawaite), REEs bearing minerals (monazite, xenotime) and accessory minerals (zircon, pyrite, galena, fluorite, apatite). Geochemically, the mylonitic rocks are enriched in incompatible elements and HFS elements (Nb, Zr and Y) and emplaced in greisen field. The melt of mylonitic rocks were originated from pelites (clay-rich sources). The present study shows that the geochemical characteristics of the mylonitic rocks could be used as exploration guides for U, Th, Nb, Zr and Ga rich sites in similar occurrences in the northern part of the Pan- African belt of Egypt. The mylonitization process led to changes in shape and size of minerals and accompanied with change in chemical compositions of the original rock. It could be related to role of the fluid, heating and metasomatic processes. Detailed spectrometric study reveals the eU/eTh ratio varies directly with eU concentration and randomly with eTh, indicating that the radioelement concentration is governed by post magmatic redistribution. The origin of these secondary minerals is mainly related to alteration of primary minerals by the action of oxidizing fluids, mobilization of uranium and then redeposition in other forms. Redistribution by circulating meteoric water might have taken place.

Key words: Mineralizations, spectrometric study, mylonites, boltwoodite, niobium.

INTRODUCTION

Wadi Sikait area located between Longitude 34° 46' to 34° 47' E and Latitude 24° 41' to 24° 43' N. The lithological constitution of Nugrus Sikait area comprises a sequence of dismembered ophiolites, tectonic mélange association and arc assemblage. These older rocks are intensively deformed and intruded by intracratonic association, which within the mapped area, are represented by gabbros and the associated hornblendite together with younger granites (Saleh, 1997). The hydrothermal base metal at Sikait area is estimated to have metamorphism and deformation in the area and intrusion of the Pan-African biotite granites and garniferous leucogranites (Ibrahim et al., 1999). The area had been studied by

many authors (Hashad, 1959; Basta and Zaki, 1961; El Shazly and Hassan, 1972; Hassan, 1973; Abdel Monem and Hurley, 1979; Surour, 1995; Mohamed and Hassanein, 1997; Saleh, 1997; Assaf et al., 2000; Hashad, 2001). Wadi Sikait is belonging to Wadi Ghadir - Wadi Hafafit fold belt which is a segment of Eastern Desert of the Arabian-Nubian shield of Pan - African orogeny. The Pan - African ophiolite and island arc assemblage were thrust from the east over the Pre-Pan - African rocks toward the west that were largely mylonitized at shallow depth or remobilized at the greater depths (El Gaby et al., 1988). Structurally, the rock units of this fold belt can be divided into two major groups separated by a low angle major thrust fault (Nugrus thrust). The hanging wall group comprises low grade metamorphic rocks of the ophiolitic mélange which cover extensive areas to the north and east the structure.

*Corresponding author. E- mail: drgehad_m@yahoo.com

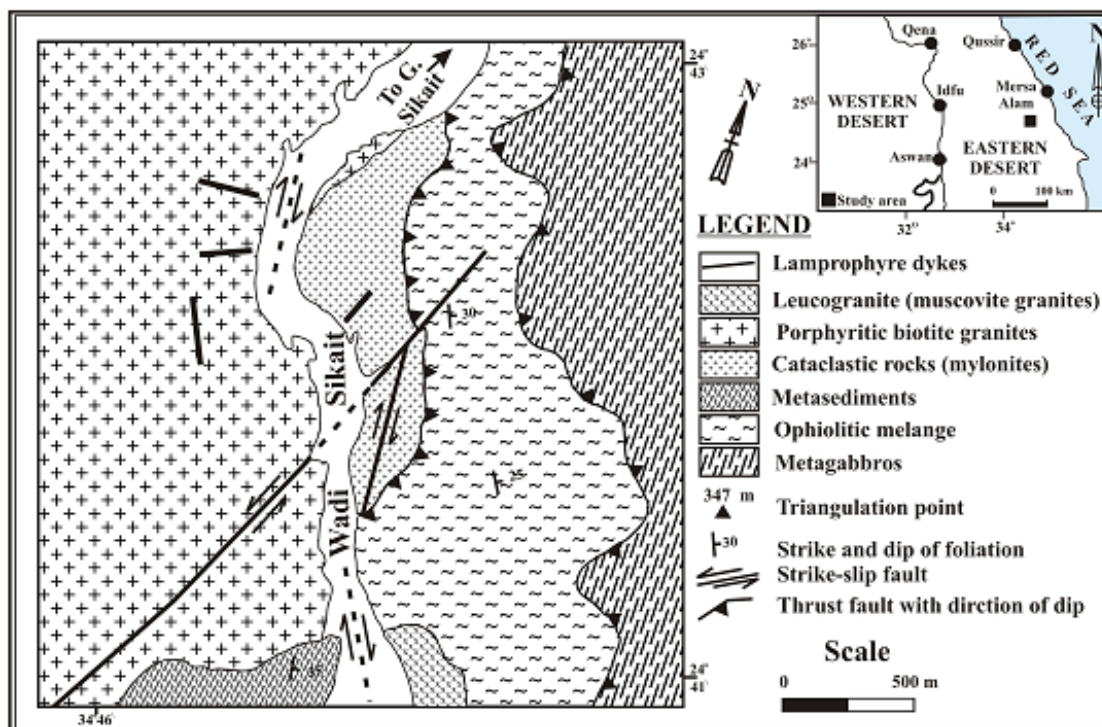


Figure 1. Geological map of Wadi Sikait area, Southeastern Desert, Egypt (Saleh, 1997).

The footwall comprises medium grade of gneisses units which form antiformal stack west the structure. Wadi Ghadir mélangé unit represent a section across a fossil deep-sea trench, accretionary and forearc (El Akhal, 1993; El Sharkawy and El Bayoumi, 1979). Wadi Hafafit probably formed a continental margin/ volcanic arc environment at the beginning orogeny Pan- African development (El Bayoumi and Greiling, 1984). Greiling et al. (1994) concluded that post collisional evolution in Eastern Desert of Egypt started with extensional collapse, which was followed by NNW-SSE shortening and related large - scale thrusting (toward the NNW) and folding, distributed all over the Eastern Desert, followed by further period of Late to Post- activity. This study throws the light on the regional geologic setting, geochemical characteristics and spectrometric prospecting of the mylonites of Wadi Sikait, Southeastern Desert of Egypt.

Geologic setting and field observations

The following is a detailed field description of the rock units at Sikait area (Figure 1)

Metagabbros

Metagabbros occur as high hills in the east sector of the

Sikait area. They are ophiolitic and thrust over ophiolitic mélangé (Saleh, 1997). The thrusting angle changes as a result of the intrusion of the muscovite granites (leucogranites) in ophiolitic mélangé. Metagabbros characterized by pockets of pegmatitic gabbros rich in feldspars (some pink in colour), anorthosites and trondhjemite. These most probably represent injections of the later differentiates of the gabbroic magma.

Ophiolitic mélangé

The ophiolitic mélangé is composed of 2% ophiolitic blocks of meta-peridotites, meta-pyroxenites and ortho-amphibolites tectonically embedded in highly pervasively deformed matrix of metasedimentary origin. Matrix rocks are schists (talc, tremolite/actinolite, sillimanite graphite, garnetiferous hornblende biotite, phlogopite, garnetiferous phlogopite and garnetiferous staurolite, Saleh, 1997). Ophiolitic mélangé is thrust over the mylonites rocks and occurs in the east Sector as strip running in NNW-SSE. The foliation is parallel to Wadi Sikait shear zone.

Metasediments

Metasediments are thrusting over mylonitic rocks and intruded by porphyritic biotite granite. They occur in the

Southwestern part of the mapped area and extend beyond it. Their foliation strikes parallel to the NNW-SSE right lateral strike slip fault of Wadi Sikait. The rocks are fine to medium-grained of greenish grey and whitish grey in colour. They are represented by meta-calc-pelites (para-amphibolites and hornblende biotite schists) and meta-psammopelites (banded muscovite biotite schist and quartzo-feldspathic biotite schist, Saleh, 1997).

Cataclastic (mylonitic) rocks

The mylonites in Wadi Sikait cover an area of about 113000 m² with the average elevation above the Wadi Sikait alluvium about 5 m. Mylonites nearly occur in the central part of eastern sector along Wadi Sikait. They are affected by two set of strike slip faults, the first is NNW-SSE right lateral, whereas the second N-S is left lateral. Mylonites are intruded by porphyritic biotite granites separating it from the Abu Rushied mylonites. The mylonitic rocks contain quartz veins result extensive recrystallization and remobilization of quartz. The wallrock alteration facies are hematitization, greisenization, silification, albitization, fluoritization and pyritization. Mylonites are fine to medium grained; they are composed mainly of quartz, alkali feldspars, plagioclase (An₇₋₁₂), biotite and riebeckite, together with zircon, apatite, allanite, titanite and opaques.

Porphyritic biotite granites

Porphyritic biotite granites are occupying the western sector of the study area. These rocks are highly sheared, shows gneissosity structure, contain xenoliths of different shape and size as well as enclaves of biotite. They are dissected by Wadi Sikait right lateral strike slip fault along east margin left lateral strike slip fault running in N-S direction and lamprophyre dykes running nearly the in E-W and NNW-SSE directions. The rocks are medium to coarse-grained pink or reddish colour with porphyritic potash feldspar crystals and composed mainly of quartz, potash feldspars and plagioclase, together with subordinate amounts of biotite, chlorite, zircon, titanite and opaques.

Leucogranites (muscovite granites)

The leucogranite at the Sikait area intruding the southern part of the ophiolitic mélangé rocks contains large xenoliths of metasedimentary rocks. These mafic xenoliths and mica pockets contain coarse grained muscovite, feldspars as well as abundant crystals of garnets. These granites commonly contain xenoliths of mafic rocks as well as mica pockets microscopically; they are composed of euhedral to subhedral alkali feldspars,

sodic plagioclase (An₆₋₁₂), quartz, muscovite and biotite. Garnet, allanite, zircon, kyanite, apatite, fluorite, ilmenite and monazite are the common accessories. The presence of garnet and muscovite flakes reflects the peraluminous nature.

Lamprophyre dykes

The lamprophyre dykes strike in the E-W, NNW-SSE and NNE-SSW directions. These rocks vary in thickness from 0.25 to 0.5 m and up to 150 m long cutting porphyritic biotite granites and mylonitic rocks. They show weak alteration and mineralization, compared with the Abu Rusheid area. Microscopically, lamprophyre is mainly composed of plagioclase, amphiboles, phlogopite and relics of pyroxenes phenocrysts embedded in fine-grained groundmass. Xenotime, fluorite, chlorite, carbonate and opaques are accessories.

MINERALOGY

Mineralogical investigation of the separated heavy minerals from two technological samples (10 kg) were carried out by binocular microscope, XRD and ESEM techniques [Model Phillips XL 30 with Energy Dispersive X-ray (EDX)] to identify uranium and associated minerals (Figures 2 and 3) in the mylonites rocks at the Nuclear Materials Authority laboratories of Egypt. Mineralogical investigation of the heavy minerals was carried out as follow: Each sample was crushed then sieved into various mesh sizes. The -60 +150 and -150 +200 mesh size fractions were concentrated using Wulffly table to remove the light mineral fraction (e. g. feldspars and quartz), then the heavy fraction was dried. The magnetite was separated by hand magnet, while the magnetite-free fraction was concentrated using bromoform (Sp. G. = 2.85). Yielded heavy fraction, passes the Frantz Isodynamic Separator at 80 side tilt and 200 forward slopes and at different current intensities (0.2, 0.5, 1.0 and 1.5 A) in order to separate the heavy minerals according to susceptibilities.

Uranium and thorium minerals

Uranium and thorium minerals in the studied mylonites include boltwoodite $K_2(UO_2)(Si_2O_2)(OH).H_2O$, uranothorite $(Th,U)SiO_4$ and thorite $(ThSiO_4)$.

Boltwoodite

Boltwoodite is secondary uranium and occurring as pale yellow radiated acicular or fibrous. It is identified by ESEM and XRD (Figure 2a and Table 1) and contains

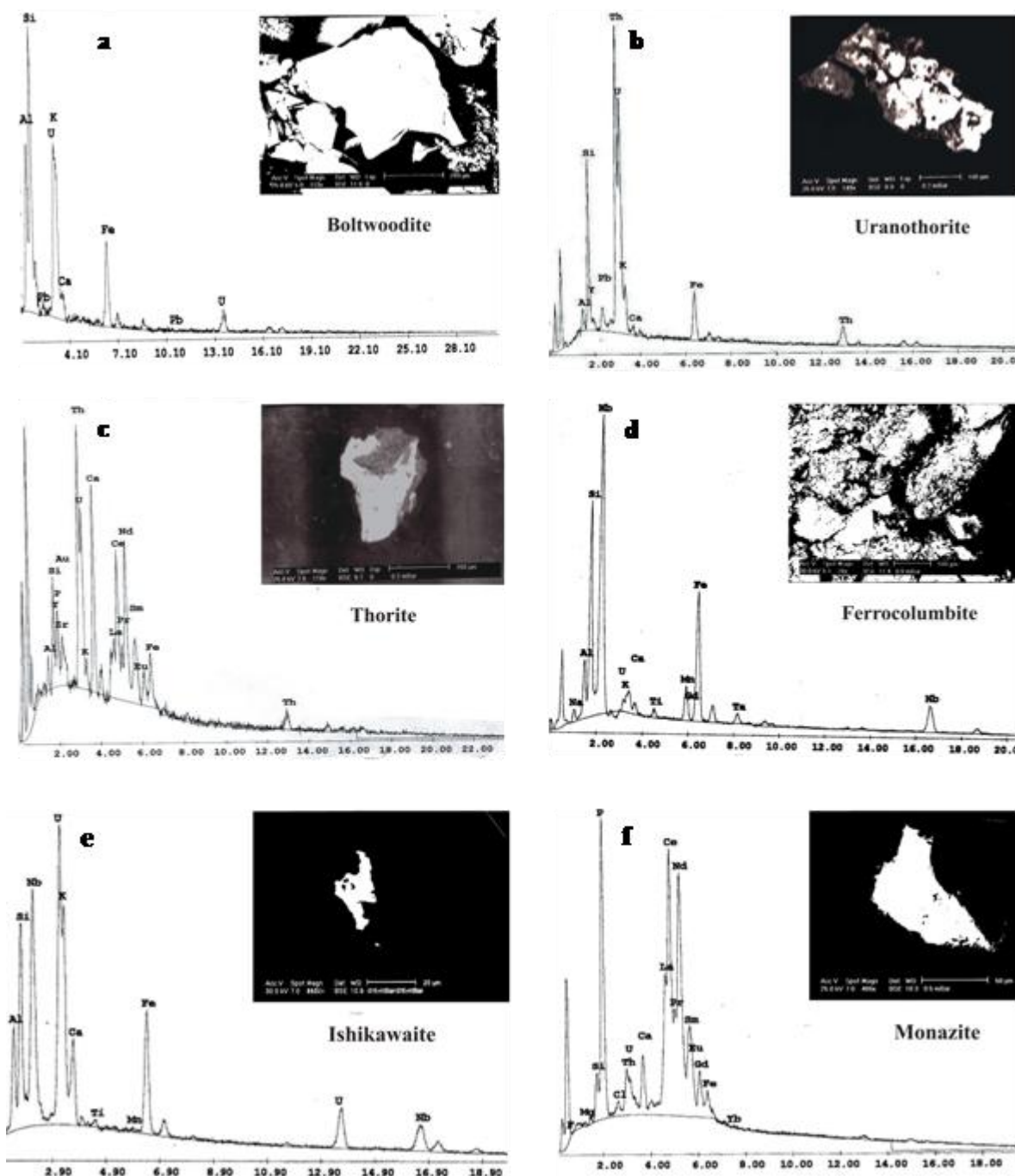


Figure 2. ESEM image and EDX analysis data of boltwoodite, uranothorite, thorite, ferrocolumbite, ishikawaite and monazite in mylonites of Wadi Sikait, Southeastern Desert, Egypt.

48.54% U, 19.24% Si and 5.21% K.

Uranothorite

Uranothorite is yellowish brown and orange in colour

associated with monazite and crystallized in cubic system with hexagonal form. It is identified and confirmed by ESEM and XRD (Figure 2b and Table 2) and contains 50.9% Th, 16.9% U and 16.14% Si. It is isostructural with thorogummite [$\text{Th}(\text{SiO}_4)_{1-x}(\text{OH})_{4x}$] and may contains as much as 10% uranium.

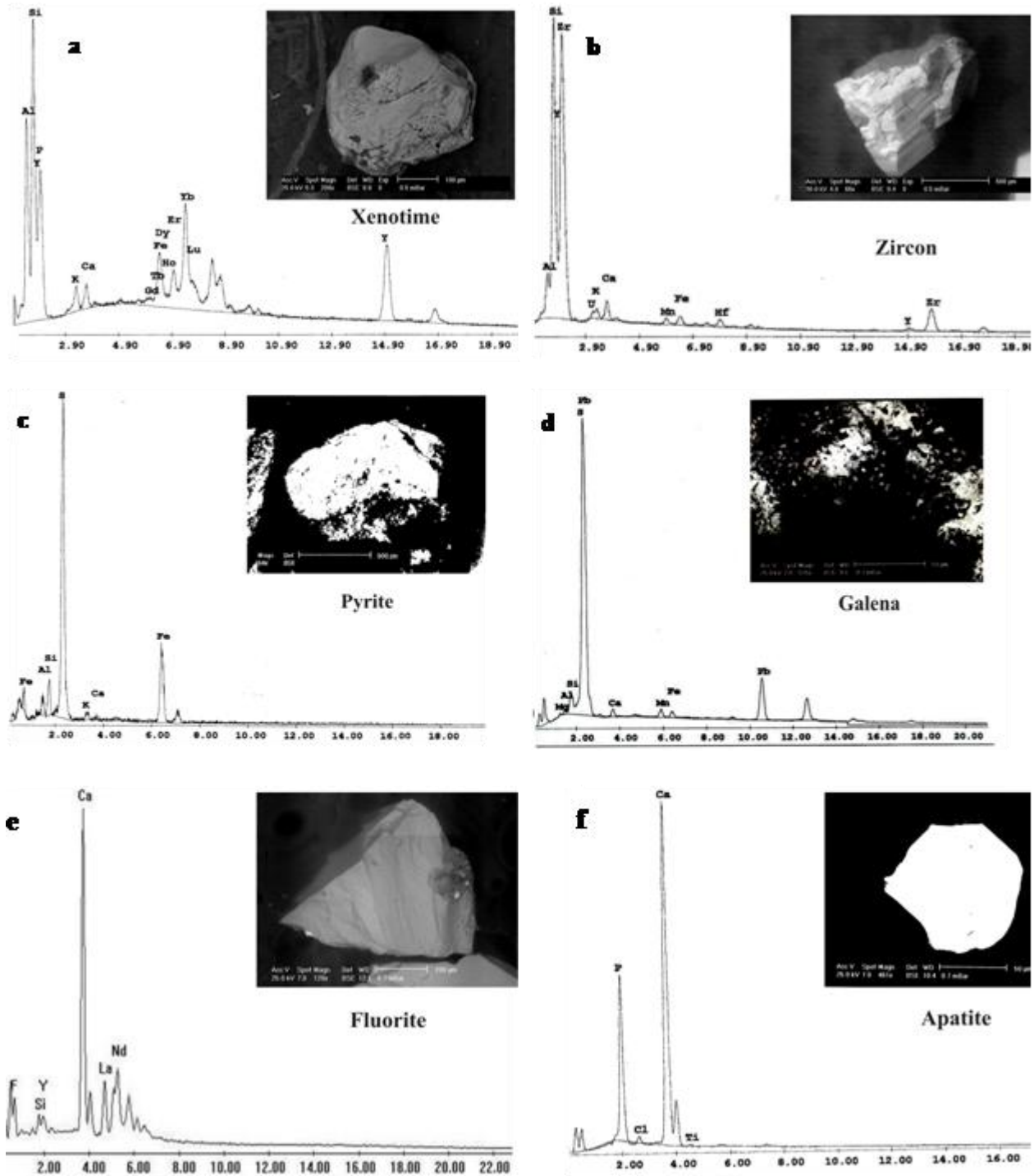


Figure 3. ESEM image and EDX analysis data of xenotime, zircon, pyrite, galena, fluorite and apatite in mylonites of Wadi Sikait, Southeastern Desert, Egypt.

Thorite

Thorite occurs as black to brownish black grains associating quartz and iron oxides minerals. Thorite grain

is less often massive which is identified by ESEM and confirmed by XRD (Figure 2c and Table 1). It contains 23.11% Th, 6.86% Si, 40.84% (La + Ce + Pr + Nd + Sm) and 6.86 %Y.

Table 1. X-ray diffraction patterns of the boltwoodite and thorite minerals for Wadi Sikait area.

Sample		Boltwoodite(8-442)*		Thorite(11-172)*	
dÅ	I/I ₀	dÅ	I/I ₀	dÅ	I/I ₀
7.90	85	7.88	100		
7.76	100				
6.61	16	6.61	40		
5.40	14	5.42	40		
5.04	5				
4.82	20	4.76	50	4.69	90
4.53	4			4.55	40
4.27	5	4.29	20		
3.93	57	3.94	90		
3.87	50			3.90	90
3.59	12	3.60	40	3.57	100
3.51	19	3.51	40	3.51	60
3.21	19	3.20	50	3.19	50
3.00	29	2.99	80	2.99	30
2.91	18	2.91	80	2.91	20
2.81	6			2.83	40
2.70	11	2.69	40		
2.63	14	2.63	50		
2.58	13	2.57	20	2.59	50
2.52	5	2.52	20		
1.97	9	1.969	70		
1.96	9			1.98	30
1.93	8			1.93	30

*ASTM card number.

Table 2. X-ray diffraction patterns of the uranothorite minerals for Wadi Sikait area.

Sample		Uranothorite (8-395)*	
dÅ	I/I ₀	dÅ	I/I ₀
6.40	4		
4.73	6	4.73	80
3.55	10	3.56	100
3.34	11		
3.25	11		
3.20	100		
3.15	99		
2.66	4	2.68	80
2.52	2	2.52	70
1.93	15		
1.82	3	1.834	100
1.65	5	1.667	60

Niobium minerals

Niobium minerals include ferrocolumbite and ishikawaite.

Ferrocolumbite (FeNbO₂)Ferrocolumbite (FeNbO₂) is belonging to columbite –

Table 3. X-ray diffraction patterns of the metamict zircon mineral for Wadi Sikait area.

Sample		Zircon (Metamict) (12-251)*	
dÅ	I/I ₀	dÅ	I/I ₀
4.48	38	2.43	5
3.37	87	3.30	100
2.55	100	2.52	5

tantalite group. It rich in iron and occurs as platy ore blocky minerals. It is identified only by ESEM (Figure 2d) and contains 48.49% Nb, 4.44% Ta and 14.34 Fe%.

Ishikawaite (U, Fe, Y, Ca) (Nb, Ta, Ti)O₄

Ishikawaite is noted for its high U-content. It closely resembles samarskite and may contain many elements by very rare ratio. This mineral identified by ESEM (Figure 2e) and contains 47.37% U, 9.73% Fe, 4.31% Ca and 25.81% Nb. The concentrations of Nb in the crust are 20 ppm (Pohl, 2009) but in the studied mylonites range from 79 to 1270 ppm with an average of 715 ppm.

REE bearing minerals

REE bearing minerals in mylonites are represented by monazite (Ce, La...) PO₄, xenotime (YPO₄) and fluorite (CaF₂).

Monazite

Monazite is monoclinic form adopted by light lanthanide or orthophosphate (Ni et al., 1995, Boatner, 2002). The structure of monazite is similar to that of zircon in several important ways. The monazite type structure is stable at either low temperature or intermediate pressure or at low pressure and intermediate temperature (Stubican and Roy, 1963). The experimental studies in AtO₄ systems (AtO₄ = compounds that are isostructure with zircon; these are the zircon group minerals) indicate that, for a given temperature, the polymorphic sequence with increasing pressure is zircon → monazite → scheelite while the polymorphic sequence at fixed pressure and increasing temperature is monazite → scheelite → zircon (Stubican and Roy, 1963). Crystals occur as brown to reddish brown prismatic or tabular grains. It sometimes has negligible amounts of Mg, Mn, Pb, Fe, Al and H₂O. This mineral is the chief source to Th and REE (especially Ce). Monazite identified by binocular microscope and contains 14.99% P, 55.56% (LREEs) as well as 5.18% Th and 1.96% U as appears by ESEM (Figure 2f).

Xenotime YPO₄

Xenotime occurs as yellowish brown, red, grey prismatic crystals. It crystallized in tetragonal system. Xenotime commonly contains small amount of REE (Er, Ce), sometimes Th, U (up to 5%), Zr (up to 3%), Sn and Si (up to 9%). Xenotime in mylonite rocks identified by binocular microscope and contains 37.96% Y, 4.13% P, HREE (up to 26.95 wt%) and 7.19% Si as appears by ESEM (Figure 3a).

Fluorite CaF₂

The fluorite is composed mainly Ca and F, occasionally contains many other impurities such as Cl, Fe, rare earth, in rare instances of U and helium. Fluorites crystallize in cubic system and occur as colorless or yellow, green blue, violet and violet black colors. The coloration is caused by the appearance of electrically neutral of Ca and F atoms in the crystal structure (Heinrich, 1959). Fluorite in Sikait mylonites occurs as colorless crystals of violet-to-violet black color crystals in the filling cavities and micro-fractures and containing 48% Ca and 45.5% F as showing by ESEM (Figure 3e).

Accessory minerals

Zircon ZrSiO₄

Sikait mylonite contains minor amounts of zircon, apatite and sulfides (pyrite and galena). Zircon contains U (average = 3.26 wt%), Hf (average = 4.71 wt%) and Y (average = 4.16 wt%) as indicated by ESEM and XRD (Figure 3b and Table 3). The occurrence of U only in zircon crystals indicates secondary hydrothermal metamorphic origin not magmatic origin. The Th/U for the metamorphic melt zircon is often (<0.01 or lower) (Hoskin and Scaltegger, 2004). It may be that is due to the presence of a fluid during metamorphic crystallization and in some cases due to differential expulsion of cations from zircon during recrystallization. Irber (1999) indicated that the Zr/HF ratios for peraluminous granites of mideastern Germany varying among (9 to 39) with lower ratios (<20) are affected by strong magmatic hydrothermal alteration. The Zr/HF ratio in common granites is about 39 (n = 327) (Erlank et al., 1978) and are mostly close to the chondritic ratio of 38 (Anders and Grevesse, 1989). Zircon crystals in the studied mylonites indicate the Zr/HF ratios 11.67 which are subjected to strong hydrothermal origin.

Sulphide minerals

b-1 - Pyrite FeS₂

Environment Scanning Electron Microscope (ESEM)

images and semi quantitative microanalyses of pyrite (FeS_2) were carried out and illustrated in Figure 3c. The semi quantitative analyses for the pyrite flame gave S = 52.5%, Fe = 46.5% and Pb = 4.8%. Pyrite forms euhedral crystals up to 0.50 cm long and is commonly found in vugs. Pyrite itself is typically replaced by later deposited sulfides such as bismuthinite, galena and chalcopyrite (Heinrich, 1959).

b-2- Galena PbS

Galena in these rocks contains 77.56% Pb and 17.11% S as appear from ESEM (Figure 3d).

c- Apatite $\text{Ca}_5(\text{PO}_4)_3(\text{F}, \text{Cl}, \text{OH})$

Apatite occurs as prismatic or tabular crystals with shades of green to grey-green, white brown, yellow black or reddish color. It has a wide range in igneous rocks as small accessory minerals. Large crystals occur in pegmatites and in some high temperature hydrothermal veins. Apatite in mylonites is confirmed semi-quantitatively by ESEM (Figure 3f) and containing 46.4% Ca and 25.44% P.

GEOCHEMISTRY

Analytical methods

Fifteen (15) samples representing the examined mylonitic rocks were chemically analyzed for their major and trace element in the Nuclear Materials Authority of Egypt. Accuracy and precision of the analytical data are monitored by international rock standards and are found to be better than 3% for major elements and within 5 to 10% for trace elements. All XRF elements were calibrated against recommended values of international standards using the data given by Govindaraju (1984). The significant trace elements were determined by X-ray fluorescence method (Philips-PW 1480 X-ray spectrometer X-unique II with automatic sample changer PW 1510). Major oxides and trace elements abundance are given in Table 4.

Rock alteration

Sikait mylonites have propylitic composition as indicated by its A-F-K (Figure 4a) components (Meyer and Hemley, 1976). Also they are greisens on the basis of its Ab-Qz-Or (Figure 4b) normative composition (Stemprok, 1979). They are plotted on the beginning of the weathering term of Nesbit and Young (1989) basing on their K_2O , Al_2O_3 and $\text{CaO} + \text{Na}_2\text{O}$ (Figure 4c). In Rb/Sr vs. Rb/Ba ratios variation diagram (Sylvester, 1998), the Wadi Sikait

mylonitic forms a linear array of decreasing Rb/Sr with Rb/Ba (Figure 5a). The distribution probably reflects the higher Rb/Sr and Rb/Ba ratios of clay-rich sources as compared to clay-poor ones. Because Sr and Ba compatible in plagioclase, where Rb is incompatible (Harris and Inger, 1992), psammite-derived melts will trend to have higher Rb/Sr and Rb/Ba than their sources. In contrast, polytic melting will leave behind residual plagioclase (Patino and Johnston, 1991). Thus pelite-derived strongly peraluminous melts do not get the same residual plagioclase boost to their Rb/Sr and Rb/Ba ratios seen in their psammite-derived counter parts. Alteration index (alteration box plot) such as the Ishikawa alteration index (AI) and chlorite carbonate-pyrite index (CCPI), have been developed to measure the intensity of sericite, chlorite, carbonate and pyrite replacement of sodic feldspars with hydrothermal alteration. Alteration box plot is used to characterize the different alteration trends and regional diagenetic alteration (Figure 5b). The mylonitic rocks are restricted to the k-feldspar and sericite field. The SiO_2 contents of this rock type are plotted against some major oxides and Pb element. The relationships are shown on the variation diagrams (Figures 6 and 7). The data points on these diagrams demonstrate the following features:

1. The mylonitic rocks exhibit positive trends, that is, Pb increase with increasing SiO_2 content, whereas K_2O , CaO , Fe_2O_3 , Al_2O_3 and Na_2O contents show variable decrease with increasing SiO_2 {($\text{Al}_2\text{O}_3 + \text{Na}_2\text{O}$ show overall decrease, $\text{K}_2\text{O} + \text{CaO}$ show moderate decrease and Fe_2O_3 shows slightly decrease)}.
2. Accordingly, the distribution of the data points on this diagram supports the suggested sedimentary origin for these rocks (Bahatia and Crook, 1986). The diagrams (Figures 8 and 9) show positive relations between Nb and eU, Nb/eU, Zr, eTh and the negative relation with Zr/Nb due to the occurrence of ishikawaite mineral as well saturation is achieved in the final hydrothermal residual melts (Kovalenko et al., 2004). The slightly positive relation between Ga and both of eU and eTh due to small amount of Ga may be present in oxides, owing to the replacement of Fe^{3+} by Ga^{5+} (Ga produced by the hydrothermal effect on aluminum bearing minerals which was camouflaged in it) and also absorbed U and Th on iron. Both of the negative and positive clustering relations between Y and eU and eTh respectively and positive clustering between Zr and eTh indicate the samples taking from zonal concentrations of hydrothermal depositions.

GAMMA RAY SPECTROMETRY

In situ gamma-ray spectrometry measurements were carried out using UG-512 spectrometer with a 7.62×7.62 cm^2 sodium iodide (Thalium) [NaI(Tl)] crystal detector. To improve results, the background radiation is measured

Table 4. Major oxides (wt %) and trace elements (ppm) composition of the Mylonites of Wadi Sikait, Southeastern Desert, Egypt.

Major oxides	1	2	3	4	5	6	7	8	9	10	11	12	13	14	15
SiO ₂	75.75	76.88	71.56	72.82	72.56	70.82	69.10	74.75	76.11	75.85	75.39	73.81	72.01	70.57	72.32
TiO ₂	0.66	0.71	0.86	0.45	0.39	0.45	0.55	0.75	0.52	0.48	0.69	0.76	0.56	0.62	0.69
Al ₂ O ₃	12.22	11.01	12.30	12.11	12.82	13.22	14.01	11.35	11.19	11.56	11.15	11.42	12.39	13.01	11.69
Fe ₂ O ₃	1.66	2.41	2.33	2.50	2.15	2.72	3.07	2.89	2.25	2.93	2.75	2.92	2.61	2.25	2.87
MgO	0.28	0.26	0.21	0.15	0.69	0.35	0.29	0.25	0.35	0.56	0.29	0.36	0.54	0.90	0.67
MnO	0.06	0.05	0.09	0.09	0.09	0.11	0.09	0.09	0.08	0.07	0.07	0.09	0.07	0.05	0.09
CaO	0.90	0.56	0.50	0.66	0.78	0.75	0.88	0.45	0.56	0.30	0.59	0.97	0.66	0.82	0.75
Na ₂ O	4.11	4.01	5.61	5.09	5.65	5.86	6.56	4.85	4.35	4.11	3.88	4.35	5.12	5.66	5.45
K ₂ O	4.15	3.22	4.86	4.30	4.15	4.11	4.45	4.36	4.01	4.15	4.75	4.32	4.19	4.89	4.61
P ₂ O ₅	0.09	0.05	0.29	0.69	0.85	0.75	0.97	0.19	0.22	0.20	0.11	0.09	0.89	0.75	0.88
L.O.I.	0.35	0.45	0.86	0.66	0.75	0.92	0.86	0.55	0.75	0.59	0.79	1.22	1.01	0.82	0.72
Total	100.23	99.61	99.62	99.52	100.88	100.06	100.83	100.48	100.39	100.80	100.46	100.31	100.05	100.41	100.74
Ba	56.00	58.00	71.00	54.00	68.00	34.00	60.00	57.00	75.00	85.00	70.00	60.00	92.00	50.00	27.00
Pb	44.00	54.00	69.00	30.00	29.00	11.00	19.00	22.00	43.00	66.00	40.00	35.00	30.00	14.00	19.00
Sr	17.00	60.00	22.00	14.00	24.00	6.00	22.00	5.00	12.00	25.00	12.00	13.00	20.00	14.00	20.00
Ga	65.00	70.00	63.00	68.00	66.00	71.00	64.00	42.00	64.00	58.00	15.00	70.00	66.00	42.00	15.00
V	5.00	4.00	3.00	4.00	4.00	3.00	3.00	4.00	4.00	3.00	4.00	3.00	3.00	2.00	5.00
Nb	590.00	1150.00	1170.00	1270.00	1045.00	930.00	345.00	79.00	1170.00	259.00	90.00	1150.00	385.00	150.00	945.00
Y	51.00	32.00	42.00	28.00	32.00	35.00	63.00	40.00	39.00	29.00	58.00	48.00	50.00	62.00	69.00
Rb	720.00	1270.00	830.00	851.00	620.00	560.00	475.00	369.00	720.00	425.00	155.00	1085.00	355.00	759.00	240.00
Zr	3120.00	2440.00	2570.00	2655.00	3210.00	2445.00	1210.00	2530.00	2530.00	1490.00	1170.00	2730.00	2745.00	1360.00	2970.00
Zn	340.00	295.00	188.00	99.00	280.00	310.00	210.00	75.00	115.00	145.00	302.00	210.00	247.00	73.00	94.00
Cu	72.00	88.00	101.00	110.00	95.00	75.00	45.00	65.00	36.00	49.00	45.00	40.00	36.00	29.00	55.00
Ni	3.00	3.00	3.00	1.00	2.00	2.00	1.00	4.00	2.00	3.00	3.00	1.00	1.00	2.00	4.00
Co	1.00	1.00	1.00	1.00	2.00	1.00	1.00	1.00	1.00	1.00	1.00	1.00	2.00	1.00	1.00
eU	49.00	105.00	50.00	62.00	68.00	79.00	20.00	85.00	270.00	56.00	30.00	90.00	15.00	85.00	54.00
eTh	72.00	290.00	121.00	288.00	30.00	110.00	50.00	270.00	310.00	33.00	20.00	130.00	35.00	110.00	120.00

over the mylonitic rocks were carried out along topographic N-S profiles. Spectrometric contour maps (Figures 10a to f) were prepared. Consequently, the relationship of the contoured radioelement pattern and the distribution of the major anomalous lithological units have formed the basis for the present interpretation. The

spectrometric data are represented on the grid system, using four isorad maps showing the radio elements eU, eTh, K%, (eU – eTh /3.5) migration map, eU/eTh and eU/K%. eU contents over mylonites range from 15 to 270 ppm with an average 75 ppm.

The contour lines of eU (Figure 10a), when

correlated with geologic map for study area, show gentle gradient at some parts of mylonites, while they show strong gradient zones over two sets of strike slip faults. The first one is right, running NNW-SSE and split from Sikait fault. The second one is left, running NNE-SSW and split into two branches at mylonites. The lowest values for eU

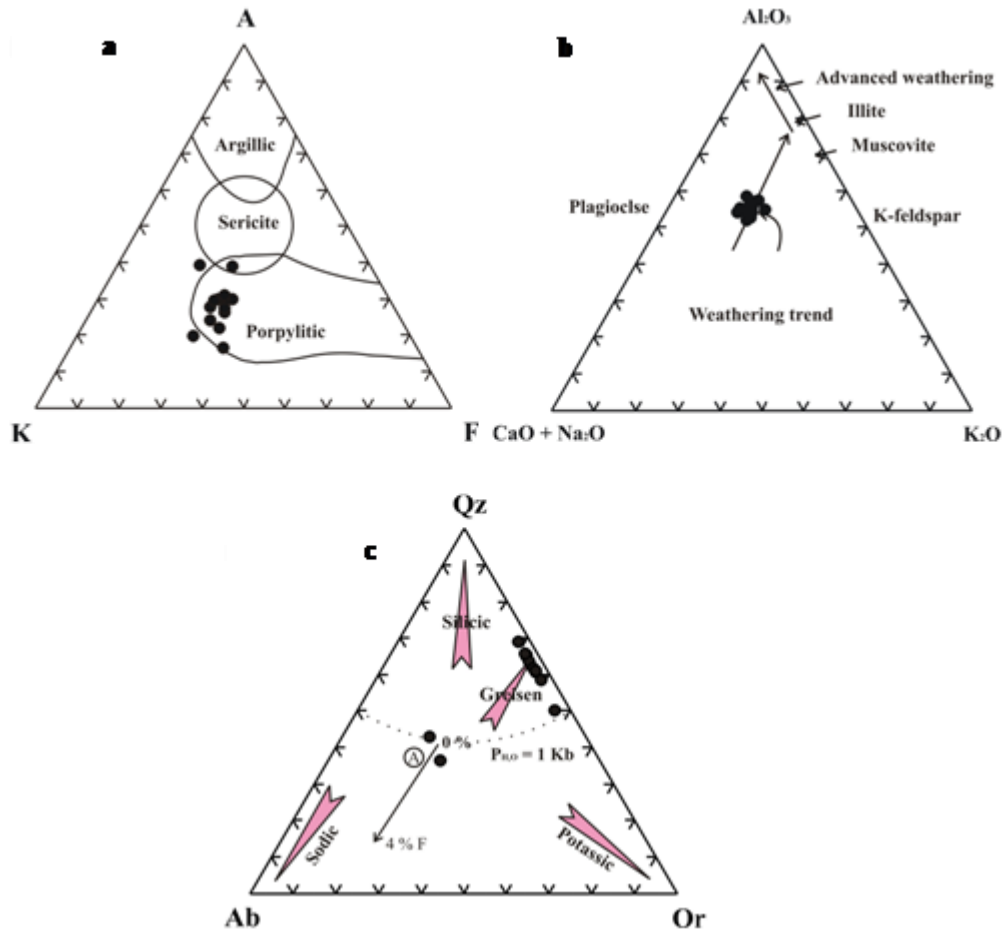


Figure 4. (a) AKF ternary diagram, after Meyer and Hemely (1967). $A = \text{Al}_2\text{O}_3 - (\text{Na}_2\text{O} + \text{K}_2\text{O})$, $K = \text{K}_2\text{O}$ and $F = \text{FeO} + \text{MnO} + \text{MgO}$, (b) $\text{Al}_2\text{O}_3 - (\text{Na}_2\text{O} + \text{K}_2\text{O}) - \text{K}_2\text{O}$ ternary diagram, showing the weathering trend, after Nesbitt and Young (1998), (c) Normative Qz - Ab - Or ternary diagram. The ternary minimum for 1kb H_2O pressure from Tuttle and Bowen (1958) and (Manning, 1981). Vector A shows the migration of ternary minima as F-content increases in the melt. The trends of granitic alteration types are from Stempok (1979), for studied mylonitic rocks of Wadi Sikait area, Southeastern Desert, Egypt.

occur above mélangé and porphyritic biotite granites. eTh contents over the mylonites range from 20 to 310 ppm with an average 133 ppm. The thorium is an immobile element and its contents remain fixed in the rock during leaching processes; the distribution of thorium can be used as geologic indicator, so, the coincidence of the contour with the lithologic ones is obvious within mylonites as shown in (Figure 10b). The correlation enrichment in eTh is coinciding with enrichment in eU (ppm). The thorium surface distribution map was useful in defining thorium enrichment zones. These zones are recommended as follow-up targets for potential having rare metals deposits (Nb). K% content over the mylonites ranges from 1.4 to 5.9 (Figure 10c). The correlation between K% and geologic map as well as surface distribution of eU and eTh in mylonites, indicate the K% increases with the decrease of eU and eTh but the other parts of mylonite are similar to the porphyritic biotite granites. The mélangé rocks show difference in the K%

contour lines especially at the central part; this may be due to the difference in minerals composition of the rock types. eU/eTh ratio is an important parameter to indicate the sites of uranium mineralization. Darnely and Ford (1989) mentioned that U/Th ratio provides the best pointers to sites where mineralizing processes most likely occur. As a rule, productive uraniumiferous rocks have U/Th ratio around one or more. U/Th ratio is also an important parameter in the detection of the oxidation state in which U is transported. Tetravalent uranium (U^{4+}) and Th can be accommodated within the same minerals, and both will be transported in solution under reducing conditions. Under oxidizing conditions, U is transported alone in the hexavalent state (U^{6+}) and usually a high U/Th ratio can be expected at the site of deposition occurs at many parts of mylonite especially at the western south part of mylonites (Figure 10d) eU/K% isorad map over the mylonites. The correlations in eU/ K% coinciding with enrichment in eU (ppm) (Figure 10e) indicate positive

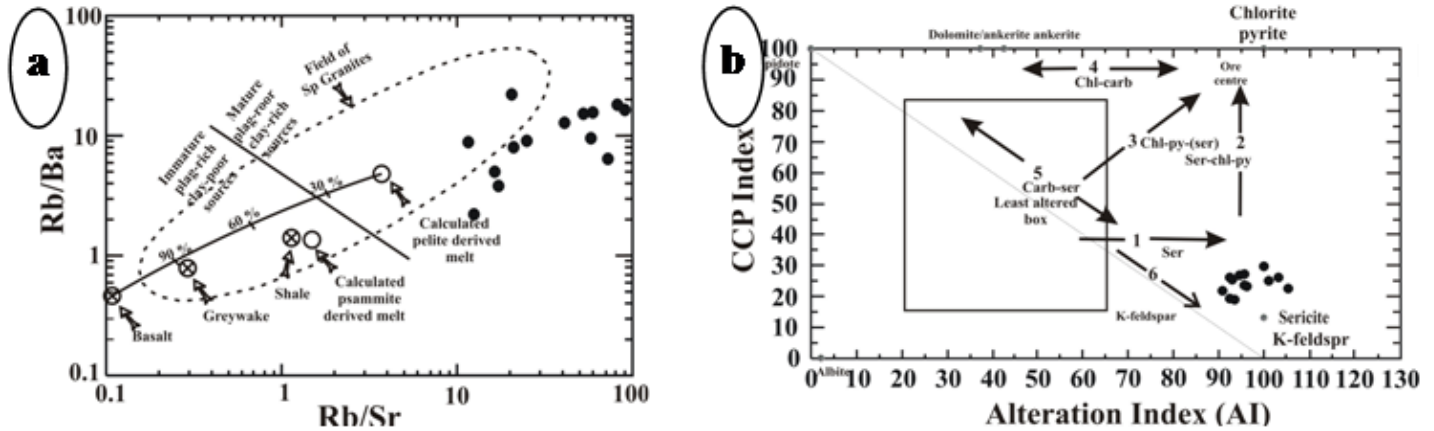


Figure 5. (a) Rb/sr vs. Rb/Ba ratio (Sylvester, 1998), for studied mylonitic rocks of Wadi Sikait area. (b) An alteration box plot with vectors for various alteration minerals (after Large et al., 2001) versus diagenetic trajectories for studied mylonitic rocks of Wadi Sikait area, Southeastern Desert, Egypt.

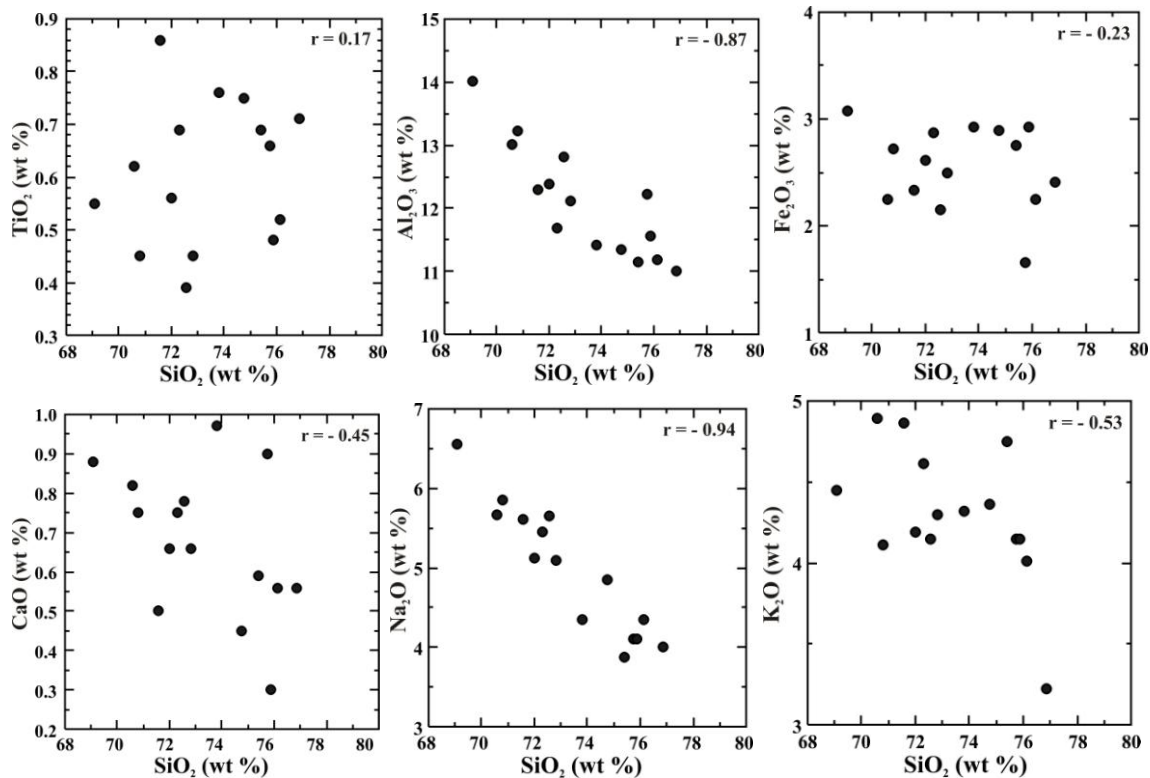


Figure 6. Variation diagrams of some major oxides against SiO₂ for studied mylonitic rocks of Wadi Sikait area.

relation. Also the lowest values occur above mélangé and porphyritic biotite granite. This result indicates the strong addition for U associated with the structures. The uranium migration map is interested in calculating the uranium mobilization; it is calculate the difference between eU now and the theoretical value (Th ppm/3.5) to give the leaching values of uranium. If this value is positive, this means that the uranium leaching in and if it negatives this mean leaching out. The U-mobility map

(Figure 10f) shows the probable trends of uranium fixation. The purple zone refers to the strong metasomatic area in the map parallel to the main structure controlled. The (eU – eTh/3.5) ratio depend mainly on the mobile element (uranium), where, (eU – eTh/3.5) = "0" (on depletion or enrichment), (eU – eTh/3.5) = "+" (enrichment) and (eU – eTh/3.5) = "-" (depletion). This ratio is important for uranium because it determined the uranium–enriched area. Enrichment in

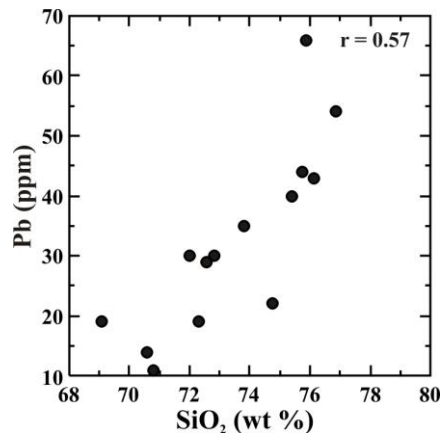


Figure 7. Variation diagram of Pb element against SiO₂ for studied mylonitic rocks of Wadi Sikait area.

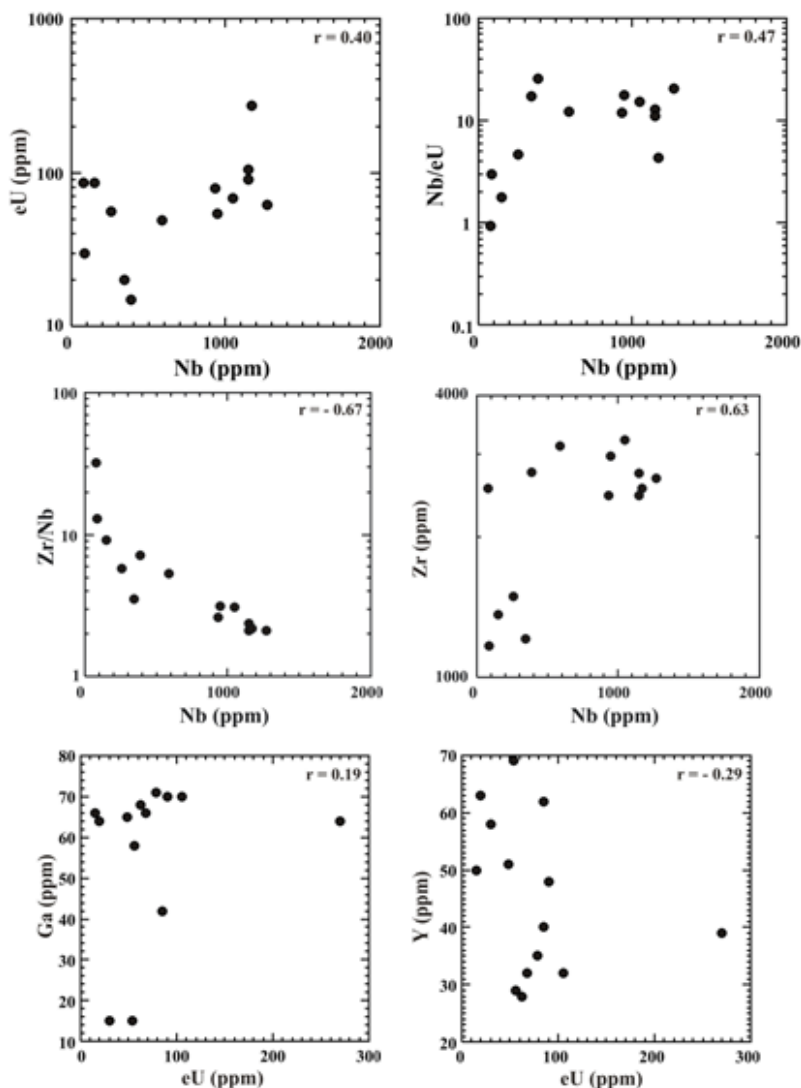


Figure 8. Binary relations between Nb and eU, Nb/eU, Zr/Nb and Zr, eU and Ga, Y for studied mylonitic rocks of Wadi Sikait area.

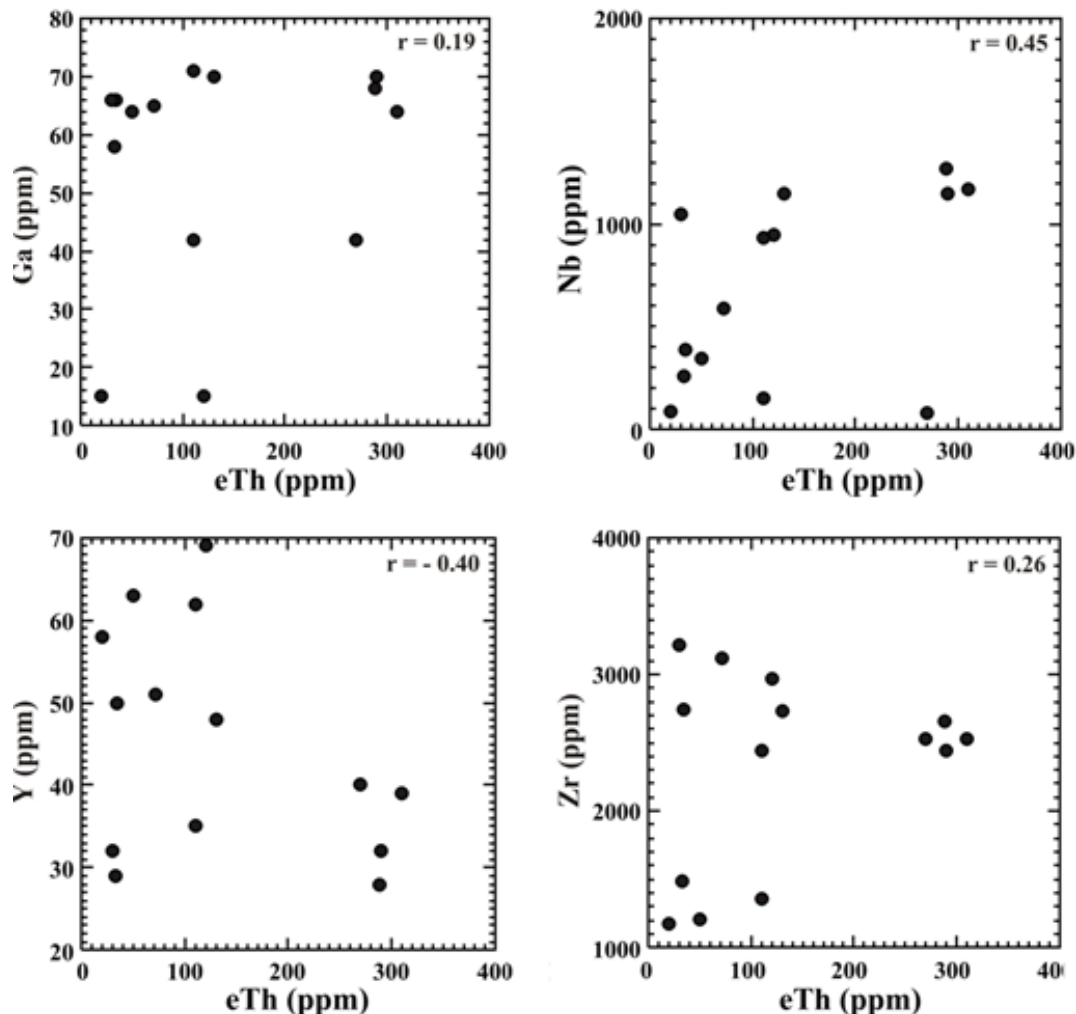


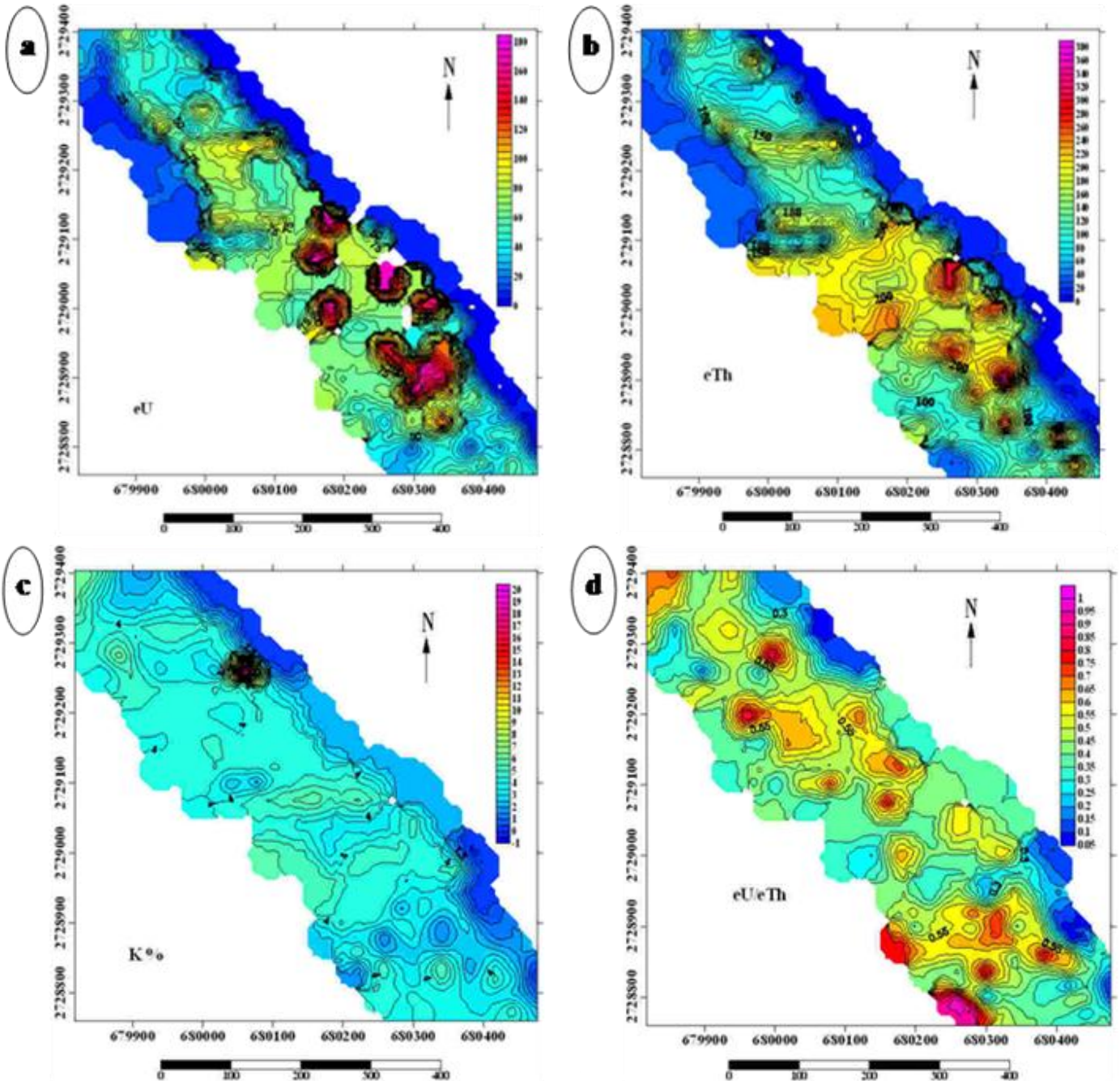
Figure 9. Binary relations between eTh and Ga, Nb, Y and Zr for Wadi Sikait area.

uranium will be indicated by an increase of this ratio, while leach out of uranium or initially uranium poor will be indicated by the decrease of it. This ratio is reaching to its maximum values over the structures, while it decreases especially along contacts with mélangé and porphyritic biotite granites.

RADIOELEMENTS DISTRIBUTION

Some variation diagrams of U and Th with their ratios have been used to indicate the mobilization of U that has been occurred within the igneous rocks (Charbonneau, 1983). Normally, Th is three times as abundant as U in natural rocks (Rogers and Adams, 1969). When this ratio is disturbed, it illustrates a depletion or enrichment of uranium. U and Th contents of granitic rocks generally increase during differentiation although in some cases they decrease (Ragland et al., 1967). Th/U ratio can either increase (Whitfield et al., 1959) or decrease

(Larsen and Gottfried, 1960) as it is controlled by the redox conditions, volatile contents, or alteration by endogens or supergene solutions (Falkum and Rose-Hansen, 1978). Relation between uranium and thorium is helpful to test if there is enrichment or depletion of these elements. Plotting eU vs eTh questioned mylonites show to the presence of thorite (Figure 11a), while most samples located along the line of eU/eTh = 0.5 and in the zone between 0.5 and 1 ratio lines indicating an enrichment of uranium rather than thorium. The positive relation between eU and eU/eTh (Figure 11b to e) means a syngenetic process with limited remobilization have controlled the U and Th distributions in the mylonitic rocks. The presence of significant uranothorite and thorite that few of samples located along the line of eU/ eTh ratio = 0.25, where thorium is enriched relative to uranium due in the studied mylonitic rocks gives more support for the syngenetic origin, whereas epigenetic process controlled the uranium distribution along the structure controlled, while weak relation between eU-K % and eTh-K%.



Tectonic evolution model

The development of the rock units in Wadi Ghadir and Wadi Hafafit fold belt formed through three stages, initially formation of volcanic arc with extensional back arc basin toward old continental and a subduction zone in the opposite direction was formed as well as normal faults in old continental. Abnormal concentrations of Nb, Ta and Be are formed along these faults (El Gaby et al., 1988). This stage followed by closure, accretion, obduction, thrusting, and formation mylonites along main

thrust fault, emplacement porphyritic biotite granites and crustal thickening with movement toward Nile Craton (Figure 12). The final extensional stage is characterized by extending crust, widespread crustal anatexis resulting in the emplacement muscovite granites (leucogranites) along major and minor thrust zones in the study area. This stage was followed by highly tectonic strike slip faults or shear zones e. g. Nugrus shear zone. A large amount of fluid is focusing along this shear zone. This fluid, namely a NaCl-dominated fluorine-bearing hydrothermal fluid that leached Zr, REEs and HFSE from

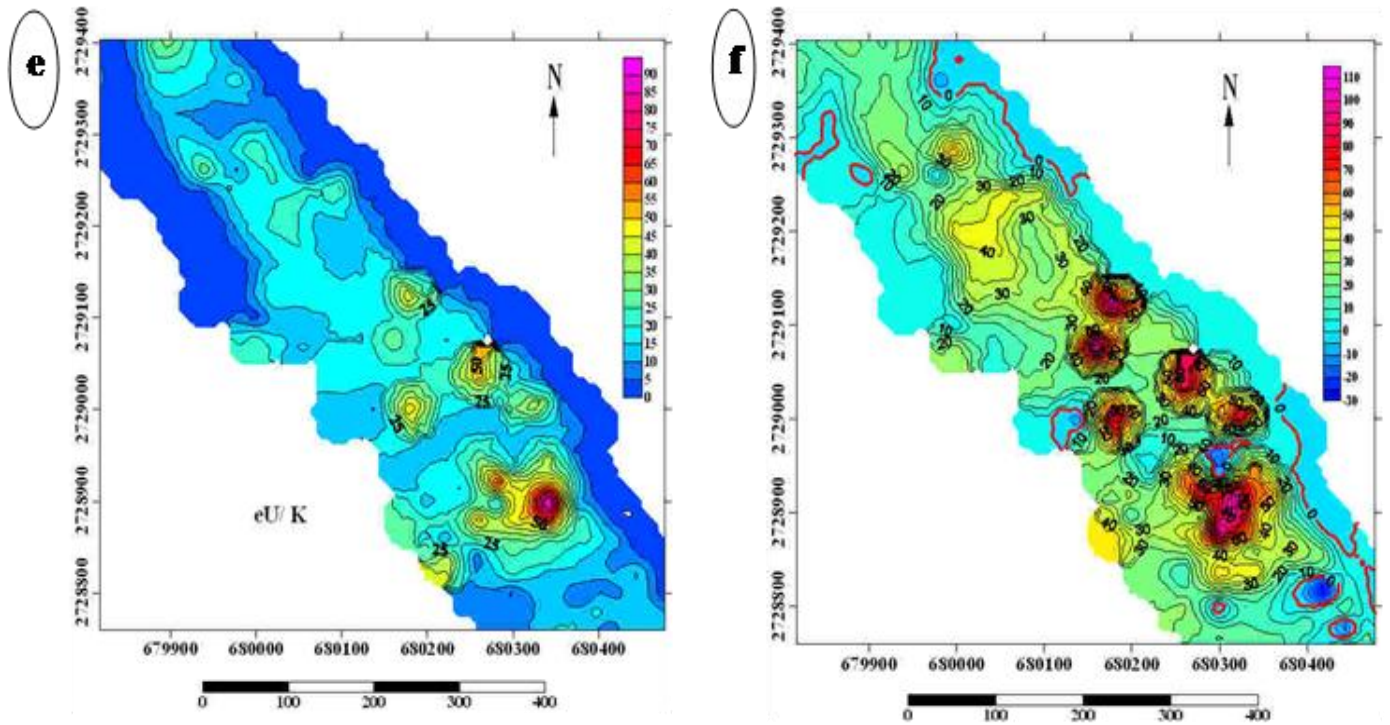


Figure 10. Contour maps showing the distribution of (a) eU, (b) eTh, (c) K%, (d) eU/ eTh, (e) eU/K% and (f) ratio, in different lithologies of the Wadi Sikait area, south Eastern Desert, Egypt.

the old continental (rich in Nb, Ta and Be) (El Gaby et al., 1988), porphyritic biotite granites (contains eU = 4 to 13 ppm and eTh = 15 to 33 ppm) and leucogranites (eU = 27 to 45 ppm, eTh = 10 to 25 ppm) (Moghazi et al., 2004, Saleh, 2008) meet with a low temperature Ca-rich fluid that originated from metagabbros and mélangé. It is proposed that the meteoric-water dominated by hydrothermal system that introduced Ca into apical parts of the mylonites and, as a result, transformed HFSE and REE-bearing minerals into Ca-bearing analogues. It is further proposed that introduction of the Ca-bearing fluid coincided with the hydrothermal fluids along Nugrus shear zone in mylonites and mixing of the two fluids led to precipitation of fluorite and destabilization of the Zr, REEs and HFSE fluoride complex due to a sharp reduction in ligand concentration and/or increase in pH. The aforementioned model explains the depletion of Zr, REEs and HFSE which accompanied the other metamorphic rocks of low temperature a long through the shear zone, and concentration of these elements in mylonites. We suggest that porosity creation initially enhanced leach of Zr, REEs and HFSE by greatly improving access of the rising hydrothermal fluid to sites containing minerals rich in these elements, and that deposition of Zr, REEs and HFSE bearing minerals only commenced when the hydrothermal fluid entered the overlying main mylonites and mixed extensively with the Ca-rich fluid circulating into the rocks from above.

DISCUSSION AND CONCLUSIONS

During mylonitization, a variable proportion of uranium in protolith rocks in refractory accessory minerals. Some of accessory minerals exhibit relatively inert chemical behavior during mylonitization and would be expected to neither lose nor gain uranium. On other hand, minerals like epidote are chemically reactive under mylonitic condition (Higgins, 1975), could either lose or gain uranium. Uranium contents increased with the initiation of brittle deformation because cataclastics and "mylonites" have an order of magnitude of more uranium than the protoliths (Coney and Reynolds, 1980). Uranium in mylonites rocks resides in number of mineralogical and structural sites, with a large proportion being concentration in structure defects and grains boundaries. Bands rich micas and migmatite of mylonitic rocks tend to be more radioelements than quartz and feldspars. Migmatite formed as a result of the action of high temperature hydrothermal fluid (bearing radioelements) on the protolith mylonites. The Wadi Ghadir and Hafafit area represents one of the important segments in the Eastern Desert of Egypt. It comprises two major groups separated by a low angle major thrust fault (Nugrus thrust). The hanging wall group comprises low grade metamorphic rocks of the ophiolitic mélangé which cover extensive areas to the north and east of the structure. The footwall comprises medium grade of gneisses units

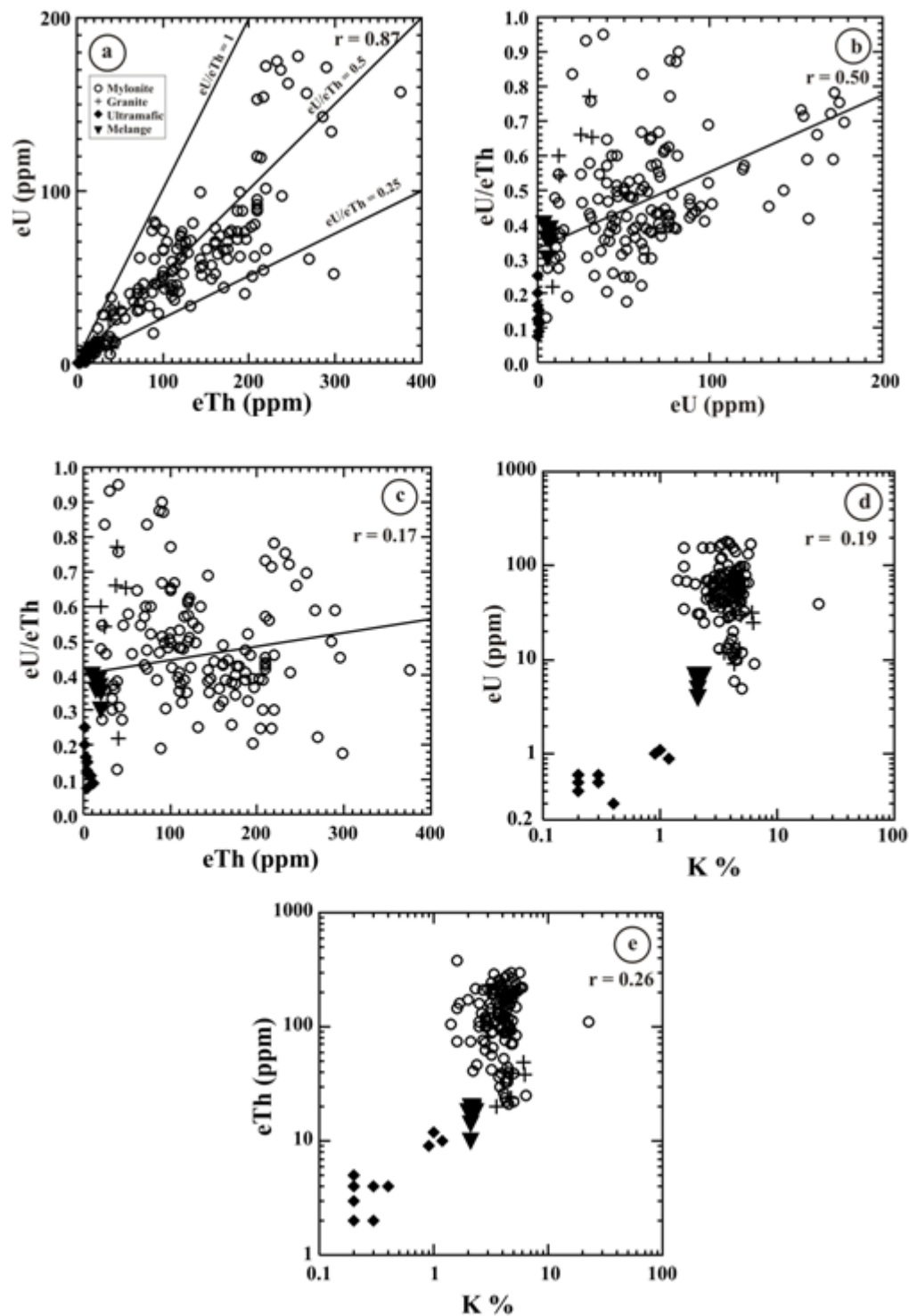


Figure 11. Binary diagrams showing (a) eU - eTh (b) eU - eU/eTh (c) eTh - eU/eTh (d) K % - eU and (e) K % - eTh in mylonites of Wadi Sikait, southeastern Desert, Egypt.

which form antiformal stack west of the structure. The study area is characterized by a distinctive relationship between sedimentation (greywackes and lithic arenite to arkose rocks in back-arc basin which metamorphosed

later to paragneisses), tectonic deformation (thrusting and folding), metamorphism (amphibolites facies in Hafafit unit, and greenschist facies in Nugrus unit), and magmatism (arc-related and collision-related granitoids).

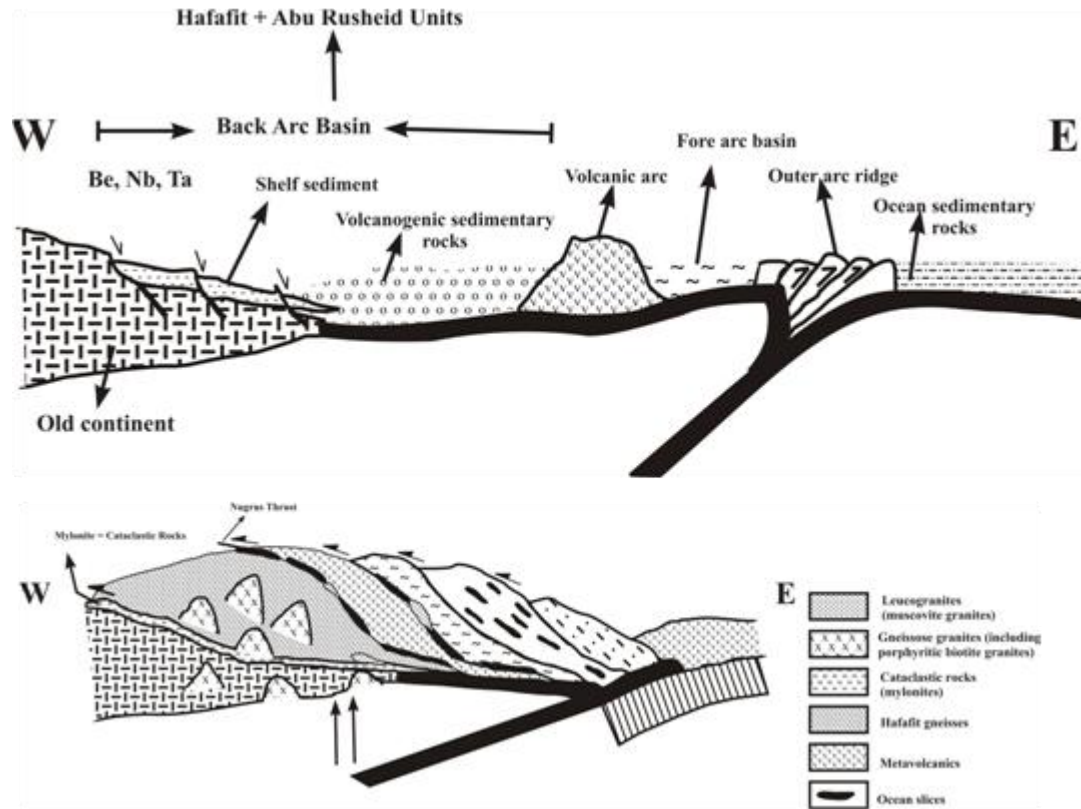


Figure 12. Evolutionary plate-tectonic model (modified after El Gaby et al., 1988, Saleh, 1997 and Abd El-Naby and Frisch, 2006).

These processes lead to development of basins, mountain building and eventual exhumation of Hafafit metamorphic complex (HMC). Such features are characteristics of orogenic belts which are located at convergent plate boundaries and along lines of arc collision (Saleh, 1997, Abd El-Naby and Frisch, 2006). The mylonite rocks are formed were the Pre Pan African rocks were subjected to dynamic metamorphism at low temperature shallow levels along the main thrust fault (Nugrus thrust fault) separating them from the overlying Pan African rocks. The magmatism in Wadi Ghadir and Hafafit area are represented by two main magma generations. The early stage of magma produced gneissose granites underplating subduction. During the final collisional stage, the metasediments underwent widespread anatexis which led to final magma producing muscovite granites. This conclusion is supported by the isotopic compositions of leucogranites of Hafafit area that suggest a metasedimentary source for these rocks (Moghazi et al., 2004). The development of leucogranites in Hafafit and Nugrus area along major and minor thrust faults reflects the role of these faults as pathways for these leucogranites. The stage of crustal extending and emplacement leucogranites was followed by highly tectonic strike slip faults or shear zones e.g. Nugrus

shear zone. A large hydrothermal fluids contains NaCl and fluorine are associated the structure and leached the Nb, U, Th, Zr and REEs from old continental (rich in Nb, Ta and Be) (El Gaby et al., 1988), porphyritic biotite granites (contains eU = 4 to 13 ppm and eTh = 15 to 33 ppm) and leucogranites (eU = 27 to 45 ppm and eTh = 10 to 25 ppm) (Moghazi, 2004; Saleh, 2008). In mylonites, these fluids meet with another fluid rich in Ca coming from the overlying metagabbros (Abu, 2007) and led finally to deposition Nb, U, Th, Zr and REEs. The high radioactive (fertile type) possess high silica content ranges from 69.1 to 76.88% with respect to alumina and enrichment in sodium and potassium (7.23 to 11.01%), besides impoverished in ferromanganese and calcium. Mylonites moreover possess high Rb and low Sr (range from 155 to 1270 ppm and 5 to 25 ppm, respectively) with an average high zirconium content range from 1170 to 3210 ppm. The above parameter can be used as indicator for the prospection on the similar mylonites. Besides, the area occurs in active region for minerals. Therefore, it could be concluded that the mylonitic rocks of high uranium favorability indices need further exploration and investigation in order to localize the most promising area of high potentiality of uranium mineralization. Thus, the surface studies on the mylonitic

rocks yield a favorable environment to form uranium deposit and the area still needs more subsurface investigation through exploratory drill holes to complete the exploration program.

ACKNOWLEDGMENTS

The authors are greatly indebted to Prof. Dr. M. El Ahmadi Ibrahim and Prof. Dr. Fawzy Siha Bakhit, who kindly made available facilities and critical comments.

REFERENCES

- Abd El-Naby H, Frisch W (2006). Geochemical constraints from the Hafafit Metamorphic Complex (HMC): Evidence of Neoproterozoic back-arc basin development in the central Eastern Desert of Egypt. *J. Afri. Earth Sci.*, 45: 173–186.
- Abdel Monem AA, Hurley PM (1979). U - Pb dating of zircons from psammitic gneisses, Wadi Abu Rusheid _ Wadi Sikait area, Egypt. *Inst. Appl. Geol., Jeddah Bull.* 3(2): 165–170.
- Abu Elatta SA (2007). Occurrence of rare metals at Gabal Abu Khruq area, South Eastern Desert Egypt. Ph.D., Faculty of Science, Ain Shams University, Egypt. P. 174.
- Anders E, Grevesse N (1989). Abundance of the elements: meteoric and solar. *Geochim. Cosmochim. Acta* 53: 197-214.
- Assaf HS, Ibrahim M E, Zalata AA, El Metwally AA, Saleh G M (2000). Polyphase folding in Nugrus – Sikait area, South Eastern Desert, Egypt. *JKAU: Earth Sci.*, 12: 1–10.
- Bahatia MR, Crook KW (1986). Trace elements characteristics of greywackes and tectonic setting discrimination of sedimentary basins. *Contrib. Mineral. Petrol.* 92: 181–193.
- Basta EZ, Zaki M (1961). Geology and mineralization of Wadi Sikait area, South Eastern Desert. *J. Geol. U. A. R.*, 5(1): 1–38.
- Boatner LA (2002). Synthesis, structure and properties of monazite, pretilite and xenotime. *Rev. Mineral Geochem.* 48: 87-121.
- Charbonneau BW (1983). Study of Radiometric three radioactive granites in the Canadian Shield: Elliot Lake Ontario, Fort Smith and Fury and Hecla, N.W. in *Uranium in granites*, ed. Y.T. Maurice, *Geol. Surv. Canada*, 81-23, pp 91-99.
- Coney PJ, Reynolds SJ (1980). Cordilleran metamorphic core complexes and their uranium favorability (Final Report), Arizona Bureau of Geology and Mineral Technology, P. 320.
- Darnely AG, Ford KL (1989). Regional airborne gamma-ray surveys, a review. *Proceeding of the 3rd Intern. Conf. Geophys. Geochem. Expl. Minerals Groundwater Ontario Geol. Surv. Spec.* 3: 229–240.
- El Akhal H (1993). A section through a late Proterozoic fore – arc domain from the Eastern Desert of Egypt. Ph.D. Thesis. Yarmouk University, Jordan. P. 196.
- EL Bayoumi RM, Greiling RO (1984). Tectonic evolution of Pan African plate margin in Southeastern Egypt- A suture zone overprinted by low angle thrusting? In: *J. Klerkx and Michot (eds.)*, *African Geology, Tervuren*, pp. 47-56.
- El Gaby S, List F, Tehrani R (1988). Geology, evolution and metallogenesis of the Pan African belt in Egypt. In: *S. El Gaby and R. O. Greiling (eds.)*, *the Pan African Belt of Northeast Africa and Adjacent Areas*. Fried. Viewring and Sohn, Braunschweig, pp 175-200.
- El Sharkawy MA, El Bayoumi RM (1979). The ophiolites of Wadi Ghadir area, Eastern Desert, Egypt. *Annal. Geol. Surv. Egypt* 9: 125-135.
- El Shazly EM, Hassan MA (1972). Geology and radioactive mineralization at W. Sikait – W. El Gemal area, South Eastern Desert, Egypt. *J. Geol.*, 16(2): 201-219
- Erlank AJ, Marchant JW, Cardoso MP, Ahrens LH (1978). Zirconium. In *Handbook of Geochemistry* (ed. K. H. Wedepohl). B-O. Springer, 2(4): 40.
- Falkum T, Rose-Hansen, J (1978). The application of the radioelement studies in solving petrological problems of the Precambrian intrusive Homme granite in the Flekkefjord area. *South Norway Geol.*, 239: 73-86.
- Govindaraju K (1984). Compilation of working values and sample description for 170 international reference samples of mainly silicate rocks and minerals. *Geostandards Newsletter, Special Issue No. 8*.
- Greiling RO, Abdeen MM, Dardir AA, El Akhal H, El Ramly MF, Kamal El Din GM, Osman A F, Rashwan AA, Rice AHN, Sadek MF (1994). A structural synthesis of the Proterozoic Arabian–Nubian Shield in Egypt. *Geol. Rundsch.* 83: 484-501.
- Harris NBW, Inger S (1992). Trace element modeling of pelite-derived granites. *Contrib. Mineral. Petrol.* 110: 46–56.
- Hashad AH (1959). Present status for radioactive minerals in Wadi El Gemal area, Eastern Desert of Egypt. Unpublished report, Geology and Raw Materials Dept., U. A. R.
- Hashad MH (2001). Chemical characteristics and genesis of Wadi Sikait tourmaline. *Egypt. Mineral.*, 13: 1 – 26.
- Hassan MA (1973). Geology and geochemistry of radioactive columbite – bearing psammitic gneiss of W. Abu Ruseid, South Eastern Desert, Egypt: *Annals of Geol. Surv., Egypt.* 3: 207–225.
- Heinrich EW (1959). *Geology of radioactive raw materials*. Mc Graw-Hill, New York, P. 654.
- Higgins MW (1975). *Cataclastic rocks* United States Government Printing office, Washington. pp 1-10.
- Hoskin W, Schaltegger U (2004). The composition of zircon and igneous and Metamorphic Petrogenesis. In: *Rev. Mineral. Geochem.* (eds. Paul. H. Ribbe & Jodi Rosso). 53: 27-55.
- Ibrahim ME, Amer TE, Saleh GM (1999). New occurrence of some nuclear materials and gold mineralization at W. Sikait area, Southeastern Desert, Egypt. First seminar on Nuclear Raw Materials and Their Technology, Cairo, Egypt, 1–3: 271-285.
- Irber W (1999). The lanthanide tetrad effect and its correlation with K/ Rb, Eu/ Eu*, Sr/ Eu, Y/ Ho and Zr/ Hf of evolving peraluminous granite suites. *Geochim. Cosmochim. Acta*, 63: 489-508.
- Kovalenko VI, Yarmolyuk VP, Kovach YA (2004). Isotope provinces, mechanisms of generation and sources of the continental crust in the central Asian mobile belt: Geological and Isotopic evidence. *J. Asian Earth Sci.* 23(5): 605 - 627.
- Large RR, Gemell JB, Paulik H (2001). The alteration box plot: A simple approach to understanding the relation between alteration mineralogy and litho-geochemistry associated with volcanic-hosted massive sulfide deposits. *Econ. Geology*. 96: 957-971.
- Larsen ES, Gottfried, D (1960). Uranium and thorium in selected suites of igneous rocks, *Amer. J. Sci.*, 258A:151-169.
- Manning DC (1981). The effect of fluorine on liquids phase relationships in the system Qz – Ab – Or with excess water at 1 kb. *Contrib. Miner. Petrol.*, V. 76: 206 - 215.
- Meyer C, Hemley JJ (1967). Wall rock alteration in geochemistry of ore deposits, H. L. Barnes, ed., New York: pp 166-235.
- Moghazi AM, Hassanen MA, Mohamed FH, Ali S (2004). Late Neoproterozoic strongly peraluminous leucogranites, south Eastern Desert, Egypt—petrogenesis and geodynamic significance. *Mineral. Petrol.* 81: 19-41.
- Mohamed FH, Hassanein MA (1997). Geochemistry and petrogenesis of Sikait leucogranite, Egypt: An example of S – type granite in a metapelitic sequence. *Geol. Rundsch* 86: 81–92.
- Nesbit HW, Young GM (1989). Formation and diagenesis of weathering profiles. *J. Geol.*, V. 97: 129 – 147.
- Ni Y, Hughes JM, Mariano AN (1995). Crystal chemistry of the monazite and xenotime structures. *Am. Mineral.* 80: 21-26.
- Patino DAE, Johnston AD (1991). Phase equilibria and melt productivity in the pelitic system: implications for the origin of peraluminous granitoids and aluminous granulites. *Contrib. Mineral. Petrol.* 107: 202 – 218.
- Ragland PC, Billing GK, Adams JAS (1967). Chemical fractionation and its relationship to the distribution of thorium and uranium in zoned granite batholiths. *Geochem. Cosmochem. Acta* 31: 17-33.
- Rogers JJW, Adams JAS (1969). Uranium and thorium. In: *Wedepohl, K. H. (ed.)*, *Handbook of geochemistry* Volume 2-3, 92-0-8 and 90-B-1 to 90-0-5, Springer-Verlag, Berlin.
- Saleh GM (1997). The potentiality of uranium occurrences in Wadi Nugrus area, South Eastern Desert, Egypt. Ph. D. Thesis Mans. Univ., P. 171.

- Saleh GM (2008). Late Neoproterozoic peraluminous granites, Southeastern Desert, Egypt: Residence of geochemistry and spectrometric prospecting. *Journal of geology of Egypt* (in press).
- Sylvester PJ (1998). Post-collisional strongly peraluminous granite. *Lithos*. 45: 29-44.
- Stemprok M (1979). Mineralization granites and their origin. *Episodes*, V. 3: 20 - 24.
- Stubican VS, Roy R (1963). High pressure scheelite-structure polymorphs of rare earth vanadates and arsenate. *Z. Kristallogr.* 119: 90-97.
- Surour AA (1995). Medium to high-pressure garnet-amphibolites from Gebel Zabara and Wadi Sikait, South Eastern Desert, Egypt. *J. Afri. Earth Sci.*, 21(3): 443–457.
- Tuttle OF, Bowen NL (1958). Origin of granite in the light of experimental studies in the system NaAlSi₃O₃ - KAlSi₃O₃ - SiO₃ - H₂O. *Geol. Soc. Am. Mineral. V.* 74:pp153.
- Whitfield JM, Rogers JJ, Adams JA (1959). The relationship between the petrology and uranium contents of some granitic rocks. *Geochem. Cosmochem. Acta*, 17: 248-271.